

## Ground-state bands of neutron-rich $^{236}\text{Th}$ and $^{242}\text{U}$ nuclei and implication of spherical shell closure at $N = 164$

T. Ishii,<sup>1,\*</sup> H. Makii,<sup>1</sup> M. Asai,<sup>1</sup> H. Koura,<sup>1</sup> S. Shigematsu,<sup>2</sup> K. Tsukada,<sup>1</sup> A. Toyoshima,<sup>1</sup> M. Matsuda,<sup>3</sup> A. Makishima,<sup>4</sup> J. Kaneko,<sup>5,†</sup> H. Toume,<sup>1,6</sup> I. Hossain,<sup>7,‡</sup> T. Shizuma,<sup>8</sup> S. Ichikawa,<sup>1</sup> T. Kohno,<sup>2</sup> and M. Ogawa<sup>5,†</sup>

<sup>1</sup>Advanced Science Research Center, Japan Atomic Energy Agency, Tokai, Ibaraki 319-1195, Japan

<sup>2</sup>Department of Energy Sciences, Tokyo Institute of Technology, Yokohama 226-8502, Japan

<sup>3</sup>Department of Research Reactor and Tandem Accelerator, Japan Atomic Energy Agency, Tokai, Ibaraki 319-1195, Japan

<sup>4</sup>Department of Liberal Arts and Sciences, National Defense Medical College, Tokorozawa, Saitama 359-8513, Japan

<sup>5</sup>Research Laboratory for Nuclear Reactors, Tokyo Institute of Technology, Meguro, Tokyo 152-8550, Japan

<sup>6</sup>College of Science, Ibaraki University, Mito, Ibaraki 310-8512, Japan

<sup>7</sup>Department of Physics, Osaka University, Toyonaka, Osaka 560-0043, Japan

<sup>8</sup>Quantum Beam Science Directorate, Japan Atomic Energy Agency, Kyoto 619-0215, Japan

(Received 26 December 2006; revised manuscript received 24 April 2007; published 10 July 2007)

The ground-state bands of the neutron-rich  $^{236}\text{Th}$  and  $^{242}\text{U}$  nuclei were established up to spin 10 and 8, respectively, by in-beam  $\gamma$ -ray spectroscopy using the ( $^{18}\text{O}$ ,  $^{20}\text{Ne}$ ) two-proton pickup reaction with a  $^{238}\text{U}$  and a  $^{244}\text{Pu}$  target. Deexcitation  $\gamma$  rays in  $^{236}\text{Th}$  and  $^{242}\text{U}$  were identified by selecting the kinetic energies of  $^{20}\text{Ne}$  using Si  $\Delta E$ - $E$  detectors. The excitation energies of the first  $2^+$  states in U and Pu isotopes have local minima at  $N \simeq 146$ , suggesting the possibility that nuclei with  $Z \simeq 92$  have a spherical shell closure of  $N = 164$ . Calculation using the Koura-Yamada single-particle potential gives an energy gap of 1.8 MeV at  $N = 164$  for  $^{256}\text{U}$ .

DOI: 10.1103/PhysRevC.76.011303

PACS number(s): 23.20.Lv, 21.10.Pc, 25.70.Hi, 27.90.+b

Shell structure plays a key role in stabilizing superheavy nuclei. At the present time, however, different magic numbers are predicted by different theories and parameters included within the theories. Most macroscopic-microscopic calculations predict the magic numbers of  $Z = 114$  and  $N = 184$  [1], while self-consistent relativistic mean field calculations predict other magic numbers, such as  $Z = 120, 126$  and  $N = 172, 184$  [1,2]. Single-particle energies in heavy- and transactinide nuclei in the deformed region give important information for predicting the shell structure of spherical superheavy nuclei, because some of the single-particle states in deformed nuclei with  $A \sim 250$  derive from the spherical single-particle states at  $A \sim 300$ . The systematic study of collective states in those deformed nuclei also gives a clue to the shell closure of spherical superheavy nuclei.

Nuclear structure for nuclei with  $Z \geq 100$  has been recently studied by in-beam  $\gamma$ -ray and isomer  $\gamma$ -ray spectroscopy coupled to the recoil mass separator [3–6] and by  $\alpha$ - $\gamma$  spectroscopy [7–9]. These nuclei are, however, limited to the proton-rich side of the  $\beta$ -stability line, because they were produced by heavy-ion fusion reactions. Nuclear structure of heavy-actinide nuclei at the neutron-rich side has been scarcely studied experimentally. We have measured in-beam  $\gamma$  rays of neutron-rich  $^{240}\text{U}$ ,  $^{246}\text{Pu}$ , and  $^{250}\text{Cm}$  nuclei produced by the ( $^{18}\text{O}$ ,  $^{16}\text{O}$ ) two-neutron transfer reactions [10–12]. In these measurements, the  $\gamma$  rays in the residual nuclei were selected by measuring outgoing  $^{16}\text{O}$  nuclei using Si  $\Delta E$ - $E$

detectors. In this Rapid Communication, we will report the results of in-beam  $\gamma$ -ray study of more neutron-rich  $^{236}\text{Th}$  and  $^{242}\text{U}$  nuclei produced by the ( $^{18}\text{O}$ ,  $^{20}\text{Ne}$ ) two-proton pickup reactions. Excited states in these nuclei have never been measured. We will discuss the possibility of the spherical shell closure of  $N = 164$  through the systematics of the excitation energies of the first  $2^+$  states in actinide nuclei and the calculation of an accurate spherical single-particle potential.

The experiments were carried out at the JAEA-Tokai tandem accelerator facility [13,14]. As for the  $^{236}\text{Th}$  experiment, a natural uranium target, 4 mg/cm<sup>2</sup> in thickness, electrodeposited on a 3  $\mu\text{m}$  aluminum foil was bombarded by a 200-MeV  $^{18}\text{O}$  beam with 0.1 particle nA. As for the  $^{242}\text{U}$  experiment, a 98% enriched  $^{244}\text{Pu}$  target, 0.7 mg/cm<sup>2</sup> in thickness, electrodeposited on a 3  $\mu\text{m}$  aluminum foil was bombarded by a 162-MeV  $^{18}\text{O}$  beam with 0.3 particle nA. The total doses of  $^{18}\text{O}$  ions were  $1.3 \times 10^{14}$  and  $4.4 \times 10^{14}$  for the  $^{236}\text{Th}$  and  $^{242}\text{U}$  experiments, respectively. Residual nuclei produced by the transfer reaction stop in the target or the aluminum backing. Most excited states up to medium-spin states have lifetimes longer than the stopping time. Therefore, the  $\gamma$  rays emitted by these states can be measured without Doppler shifts.

Outgoing nuclei were detected with four sets of Si  $\Delta E$ - $E$  detectors of 20 mm in diameter. These Si  $\Delta E$ - $E$  detectors were placed at a distance of 5 cm from the target, at 28° to the beam axis for the  $^{236}\text{Th}$  experiment and at 40° for the  $^{242}\text{U}$  experiment; these angles are slightly smaller than the grazing angles. The  $\Delta E$  detectors were surface-barrier Si detectors made from an ELID (ELectrolytic In-process Dressing)-grinding Si wafer. The thicknesses of the  $\Delta E$  detectors were 83  $\mu\text{m}$  and 75  $\mu\text{m}$  for the  $^{236}\text{Th}$  and  $^{242}\text{U}$  experiments, respectively.

\*ishii.tetsuro@jaea.go.jp

†Present address: Department of Radiological Sciences, Komazawa University, Setagaya, Tokyo 154-8525, Japan.

‡On leave from Department of Physics, Shah Jalal University of Science and Technology, Sylhet 3114, Bangladesh.

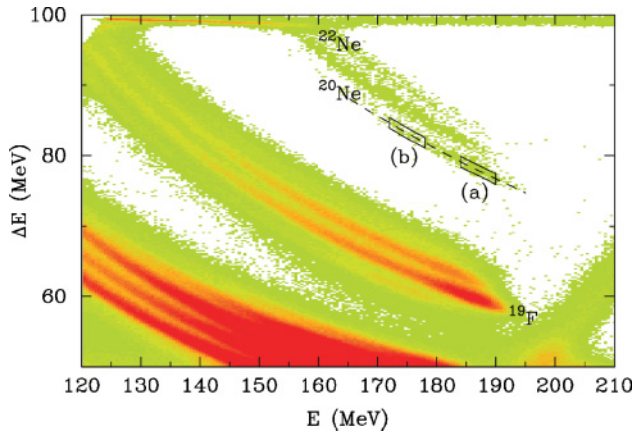


FIG. 1. (Color online)  $E$ - $\Delta E$  plot of scattered nuclei measured by a Si  $\Delta E$ - $E$  detector in the reaction of a 200-MeV  $^{18}\text{O}$  beam with a  $^{238}\text{U}$  target. The dashed line represents a calculated energy loss for  $^{20}\text{Ne}$  nuclei. See the caption of Fig. 2 for the enclosed areas (a) and (b).

Deexcitation  $\gamma$  rays in coincidence with the outgoing nuclei were measured by Ge detectors surrounding the target; seven Ge detectors were employed for the  $^{236}\text{Th}$  experiment and six detectors for the  $^{242}\text{U}$  experiment. Four Ge detectors, with 60% relative efficiency, were arranged symmetrically in the plane perpendicular to the beam axis, at a distance of 6 cm from the target. The remaining two or three Ge detectors with 30–40% relative efficiency were placed between the former Ge detectors. The absolute efficiencies of the total Ge detectors were about 3% for a 1.33-MeV  $\gamma$  ray.

An  $E$ - $\Delta E$  plot obtained from the  $^{236}\text{Th}$  experiment is shown in Fig. 1. The dashed line in Fig. 1 represents a calculated energy loss for  $^{20}\text{Ne}$  nuclei. The distribution of  $^{20}\text{Ne}$  was distinguished from those of Ne isotopes with different mass numbers. When the  $^{20}\text{Ne}$  nucleus is emitted in the transfer reaction, the residual nucleus is  $^{236}\text{Th}$ . The sum of excitation energies of scattered and residual nuclei,  $E_x$ , is derived from the kinetic energy of  $^{20}\text{Ne}$ ; a lower kinetic energy of  $^{20}\text{Ne}$  corresponds to higher  $E_x$ . The region (a) in Fig. 1 corresponds to  $E_x$  between 5 and 11 MeV. By taking coincidence with  $^{20}\text{Ne}$  within the region (a), we have observed almost equally spaced transitions of 112, 169, 224, and 273 keV as shown in Fig. 2(a). They are the candidates for the ground-state band transitions in  $^{236}\text{Th}$ . We have observed no distinct  $\gamma$  rays in coincidence with  $^{20}\text{Ne}$  having larger kinetic energies than the region (a). Since the two-proton pickup reaction has a highly negative  $Q_{\text{eff}}$  value [15], proton transfer to excited states with large angular momentum in  $^{20}\text{Ne}$  would be favored for satisfying matching condition of angular momentum. Thus, the  $\gamma$  rays in  $^{236}\text{Th}$  may not be observed at  $E_x < 5$  MeV. This fact is in contrast to the results of the ( $^{18}\text{O}$ ,  $^{16}\text{O}$ ) stripping reaction where the  $\gamma$  rays in residual nuclei were observed in the range of  $E_x$  between 0 and 6 MeV [10–12].

To confirm the assignment of  $\gamma$  rays in  $^{236}\text{Th}$ , we have examined the  $\gamma$  rays in coincidence with  $^{20}\text{Ne}$  having lower kinetic energies than the region (a). Gates of  $^{20}\text{Ne}$  were set by dividing the  $^{20}\text{Ne}$  distribution into 6 MeV in width; this energy corresponds to a neutron separation energy of  $^{236}\text{Th}$ .

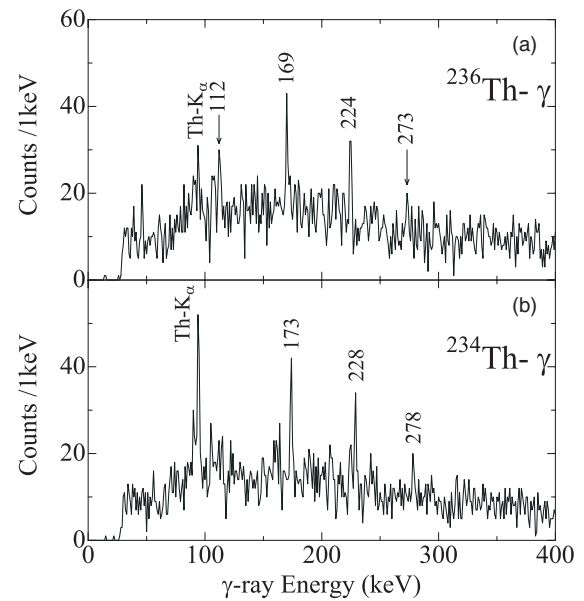


FIG. 2.  $\gamma$ -ray spectra obtained by setting the gates on  $^{20}\text{Ne}$  whose kinetic energies correspond to  $E_x$  of (a) 5–11 and (b) 17–23 MeV, respectively. These gates are depicted as the regions (a) and (b) in Fig. 1, respectively.  $\gamma$  peaks labeled by energies in the spectra of (a) and (b) are the transitions in  $^{236}\text{Th}$  and  $^{234}\text{Th}$ , respectively.

In the next gate of the region (a), the candidates for  $\gamma$  rays in  $^{236}\text{Th}$  were hardly observed. In the succeeding gate, depicted as the region (b) in Fig. 1, previously identified  $\gamma$  rays in  $^{234}\text{Th}$  appeared [16,17]. Figure 2(b) shows the  $\gamma$ -ray spectrum coincident with the region (b). Because  $E_x$  for the region (b) is higher than that for the region (a) by 12 MeV, the  $^{236}\text{Th}$  nucleus is excited high enough to evaporate two neutrons at the region (b). This observation of  $\gamma$  rays in  $^{234}\text{Th}$  suggested that the  $\gamma$  rays coincident with the region (a) are the deexcitation  $\gamma$  rays in  $^{236}\text{Th}$ . The yield of  $^{236}\text{Th}$  produced by the two-proton pickup reaction was two orders of magnitude smaller than that of  $^{240}\text{U}$  produced by the two-neutron stripping reaction. The cross section of  $^{236}\text{Th}$  was on the order of  $\mu\text{b}$ .

Following the same analysis, we have identified  $\gamma$  rays in  $^{242}\text{U}$  produced by the  $^{244}\text{Pu}(^{18}\text{O}, ^{20}\text{Ne})$  reaction. Figure 3

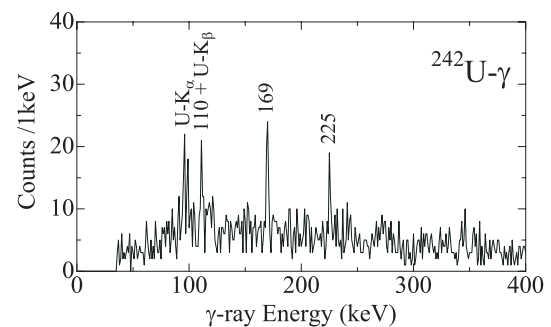


FIG. 3.  $\gamma$ -ray spectrum of  $^{242}\text{U}$  measured in the reaction of a 162-MeV  $^{18}\text{O}$  beam with a  $^{244}\text{Pu}$  target. This spectrum was obtained by setting the gate on  $^{20}\text{Ne}$  whose kinetic energies correspond to  $E_x$  between 5 and 11 MeV.  $\gamma$  peaks labeled by energies are the transitions in  $^{242}\text{U}$ .

TABLE I.  $\gamma$ -ray energies and relative intensities in  $^{236}\text{Th}$  and  $^{242}\text{U}$ . Total internal conversion coefficients  $\alpha_T$  for  $E2$  transitions were taken from Ref. [18].

$I_i \rightarrow I_f$	$^{236}\text{Th}$		$^{242}\text{U}$	
	$E_\gamma$ (keV)	$I_\gamma(1 + \alpha_T)$	$E_\gamma$ (keV)	$I_\gamma(1 + \alpha_T)$
$2^+ \rightarrow 0^+$	48.4(3) <sup>a</sup>		47.8(3) <sup>a</sup>	
$4^+ \rightarrow 2^+$	111.6(5)	240(70)	110.4(6)	170(70)
$6^+ \rightarrow 4^+$	169.4(3)	100(22)	169.3(3)	100(20)
$8^+ \rightarrow 6^+$	224.0(3)	48(12)	224.7(3)	44(14)
$10^+ \rightarrow 8^+$	272.7(5)	32(14)		

<sup>a</sup>The energy was derived from the moment of inertia deduced from the higher levels.

shows the  $\gamma$  rays in coincidence with  $^{20}\text{Ne}$  with the kinetic energies corresponding to  $E_x$  between 5 and 11 MeV. We have assigned the 110, 169, and 225 keV  $\gamma$  rays to deexcitation  $\gamma$  rays in  $^{242}\text{U}$ . The  $\gamma$ -ray energies and intensities in  $^{236}\text{Th}$  and  $^{242}\text{U}$  are summarized in Table I. Assuming that those  $\gamma$  rays form the ground-state rotational bands, we have established level schemes of  $^{236}\text{Th}$  and  $^{242}\text{U}$  up to spin 10 and 8, respectively, as shown in Fig. 4; the  $2^+ \rightarrow 0^+$   $\gamma$  transitions were not observed owing to large internal conversion coefficients,  $\alpha_T > 300$  [18].

The moments of inertia for the ground-state band of  $^{242}\text{U}$  are plotted as a function of squared rotational frequency in Fig. 5.  $\mathcal{I}^{(1)}$  and  $\mathcal{I}^{(2)}$  represent the kinematic and dynamic moments of inertia, and  $\omega$  is rotational frequency [10,12]. The  $\mathcal{I}^{(1)}$  values were derived from the spins assigned above as well as the  $\gamma$ -ray energies (Table I). The solid line in Fig. 5 is the fit of  $\mathcal{I}^{(1)}$  to  $J_0 + \omega^2 J_1$ , where  $J_0$  and  $J_1$  are constants. The  $\mathcal{I}^{(2)}$  values calculated by  $J_0 + 3\omega^2 J_1$ , drawn as the dashed line in Fig. 5, are in good agreement with the experimental ones. This fact suggests that the spin assignments of the levels in  $^{242}\text{U}$  are correct. From the  $J_0$  and  $J_1$  values, the  $2^+$  energies were deduced to be 48.4(3) and 47.8(3) keV for  $^{236}\text{Th}$  and  $^{242}\text{U}$ , respectively. These  $2^+$  energies are very precise, which would be difficult to be attained by other measurements.

The excitation energies of the  $2^+$  states in the ground-state bands,  $E_{2^+}$ , are plotted versus neutron number in Fig. 6 for even-even actinide nuclei whose excitation energies are known precisely [3,10–12,19–23]; five data for

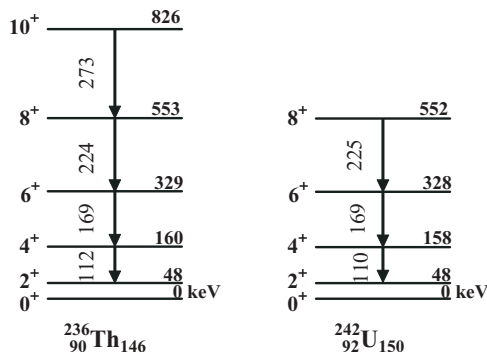


FIG. 4. Level schemes of  $^{236}\text{Th}$  and  $^{242}\text{U}$ . The  $\gamma$ -ray and level energies are in units of keV.

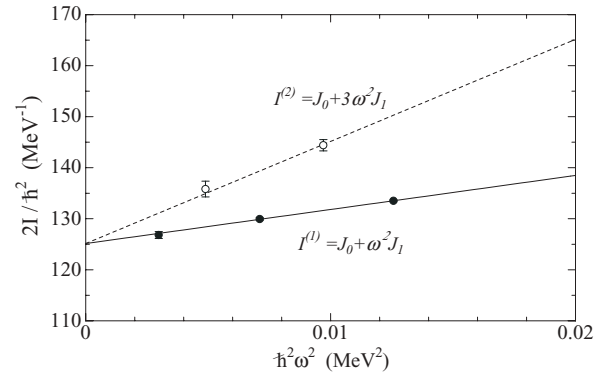


FIG. 5. Plot of moments of inertia for the ground-state band of  $^{242}\text{U}$  versus squared rotational frequency  $\omega^2$ . The closed and open circles represent the kinematic moments of inertia  $\mathcal{I}^{(1)}$  and the dynamic moments of inertia  $\mathcal{I}^{(2)}$ , respectively. The solid line is the fit of  $\mathcal{I}^{(1)}$  to  $J_0 + \omega^2 J_1$ . The dashed line is calculated by  $J_0 + 3\omega^2 J_1$ , using  $J_0 = 62.6(2)\hbar^2 \text{ MeV}^{-1}$  and  $J_1 = 334(23)\hbar^4 \text{ MeV}^{-3}$  obtained from the fit of  $\mathcal{I}^{(1)}$ .

$^{236}\text{Th}_{146}$ ,  $^{240,242}\text{U}_{148,150}$ ,  $^{246}\text{Pu}_{152}$ , and  $^{250}\text{Cm}_{154}$  were obtained from a series of our studies. In this systematics, the  $E_{2^+}$  values of Th and U isotopes have dips at  $N = 142$ . Furthermore, the  $E_{2^+}$  values of No isotopes decrease at  $N = 152$ . These sharp decreases of  $E_{2^+}$  are related to the deformed shell gaps. At the deformed shell gap, the pairing energy gap becomes smaller, resulting in a larger moment of inertia. In fact, there are deformed shell gaps at  $N = 142$  [24,25] and 152 [25–27]. In Ref. [12], we have discussed the relation between the moments of inertia of Cm isotopes and the deformed shell gap at  $N = 152$ . The disappearance of this gap for Pu isotopes will also be discussed in another paper [11]. By disregarding the dips at the deformed shell gaps, we have found that the  $E_{2^+}$  values vary smoothly and have local minima at  $N \simeq 146$  for U and Pu isotopes, and possibly for Th and Cm isotopes.

From a simple perspective on nuclear structure, we can consider that nuclei in the middle of the spherical shell closures have maximum collectivity, and thus, the excitation energies of the first  $2^+$  states may have local minima there. In fact,

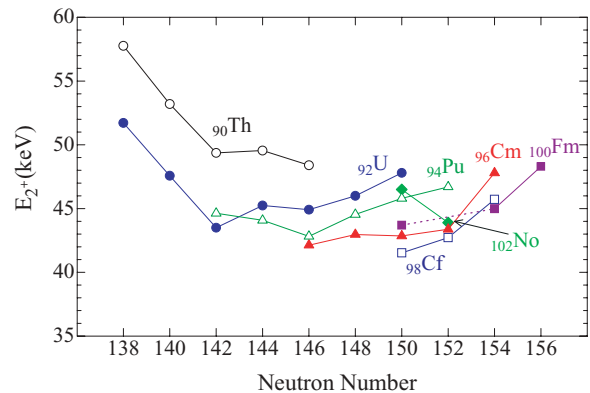


FIG. 6. (Color online) Systematics of the first  $2^+$  energies of even-even actinide nuclei. The data for  $^{250}\text{Fm}$  and  $^{254}\text{Fm}$  are connected by a dotted line because there are no accurate measurements for  $^{252}\text{Fm}_{152}$ .

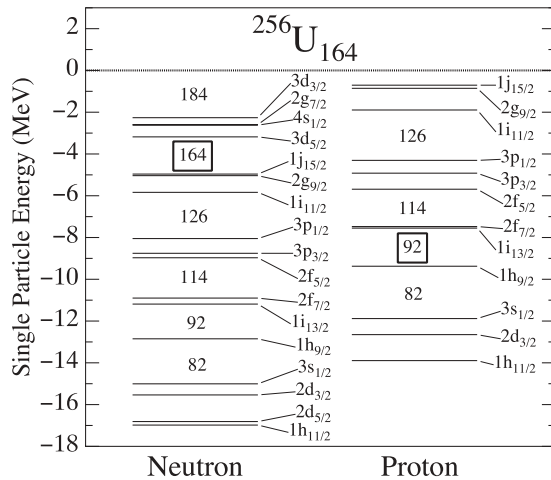


FIG. 7. Single-particle levels calculated by the KY potential for  $^{256}\text{U}_{164}$ .

this perspective is broadly true in other deformed regions. In the actinide region, one side of the spherical shell closure of neutrons is  $N = 126$ . Therefore, the other side of the spherical shell closure becomes  $N = 166$  by regarding  $N = 146$  as the middle point. Among the single-particle levels lying around  $N = 166$ , it is very plausible that there is a shell gap at  $N = 164$  between the  $1j_{15/2}$  orbital and the  $3d_{5/2}$  or  $2g_{7/2}$  orbitals. This gap is similar to the  $N, Z = 50$  gap lying between the  $1g_{9/2}$  orbital and the  $2d_{5/2}$  or  $1g_{7/2}$  orbitals. Furthermore, protons may have a spherical subshell closure of  $Z = 92$ , where the  $h_{9/2}$  orbital is fully occupied. Therefore, the  $^{256}\text{U}$  nucleus with  $Z = 92$  and  $N = 164$  may have a doubly shell closure.

The macroscopic-microscopic calculation using a multidimensional deformation space [28] reproduced and predicted the  $E_{2+}$  values of heavy- and transactinide nuclei very well. The  $E_{2+}$  values of  $^{232,234,236}\text{Th}$  were calculated as 47.3, 46.9, and 46.5 keV (experimental energies are 49.4, 49.6, and 48.4 keV), respectively, and those of  $^{238,240,242}\text{U}$  were calculated as 43.7, 44.9, and 48.0 keV (experimental energies are 44.9, 46.0, and 47.8 keV), respectively. Their calculation also well reproduced the correlation between the  $E_{2+}$  values and the deformed shell gap at  $N = 152$ . They, however, did not

mention nuclear structure of more neutron-rich nuclei around  $^{256}\text{U}$ .

Calculation using the Koura-Yamada (KY) single-particle potential [29] shows that shell gaps appear at  $N = 164$  and  $Z = 92$  for  $^{256}\text{U}$ , as shown in Fig. 7. This potential is an extension of Woods-Saxon potential including two new parameters modifying the surface structure of the potential. This potential is expressed as a smooth function of  $Z$  and  $N$ , and the potential parameters are fixed by comparison with single-particle levels in the vicinities of 15 doubly magic or magic-submagic nuclei ranging from  $^4\text{He}$  to  $^{208}\text{Pb}$ . Because this potential is very accurate and applicable to a wide region of nuclides [29], the KY potential is expected to have more predictive power than a simple Woods-Saxon potential. The KY potential gives a shell gap of 1.8 MeV at  $N = 164$  and 1.8 MeV at  $Z = 92$  for  $^{256}\text{U}$ . These energy gaps are comparable size to those calculated by the KY potential for an expected doubly-magic superheavy nucleus of  $^{298}114$  (2.5 MeV at  $N = 184$  and 1.6 MeV at  $Z = 114$ ), and are about half of those for a typical doubly magic nucleus of  $^{208}\text{Pb}$ . In the calculation of the KTUY mass formula [30] using the KY potential, it is also predicted that nuclei around  $^{256}\text{U}$  are almost spherical. Note that the Woods-Saxon potential using ‘universal parameters’ [31], which is often used for the calculations of energy levels in heavy- and transactinide nuclei [5,28,32], gives a smaller energy gap of 1.1 MeV at  $N = 164$  for  $^{256}\text{U}$  than the KY potential.

In conclusion, we have measured deexcitation  $\gamma$  rays in the neutron-rich  $^{236}\text{Th}$  and  $^{242}\text{U}$  nuclei for the first time. These nuclei were produced by the ( $^{18}\text{O}$ ,  $^{20}\text{Ne}$ ) two-proton pickup reactions, and their  $\gamma$  rays were identified by taking coincidence with  $^{20}\text{Ne}$  nuclei and selecting their kinetic energies, using Si  $\Delta E$ - $E$  detectors. We have found that the excitation energies of the first  $2^+$  states in U and Pu isotopes have local minima at  $N \simeq 146$ , disregarding the  $E_{2+}$  value of  $^{234}\text{U}$  having the deformed shell closure of  $N = 142$ . A spherical shell closure of  $N = 164$  is expected for nuclei with  $Z \simeq 92$ , which would also affect the prediction of the path of the r-process for heavy nuclei.

We acknowledge the staff of the tandem accelerator for operating it at the highest terminal voltage of 18 MV. I.H. was supported financially by BK21 and JSPS.

- [1] A. Sobczewski and K. Pomorski, *Prog. Part. Nucl. Phys.* **58**, 292 (2007).
- [2] A. V. Afanasjev, T. L. Khoo, S. Frauendorf, G. A. Lalazissis, and I. Ahmad, *Phys. Rev. C* **67**, 024309 (2003).
- [3] R.-D. Herzberg, *J. Phys. G* **30**, R123 (2004).
- [4] P. Reiter *et al.*, *Phys. Rev. Lett.* **95**, 032501 (2005).
- [5] S. K. Tandel *et al.*, *Phys. Rev. Lett.* **97**, 082502 (2006).
- [6] R.-D. Herzberg *et al.*, *Nature (London)* **442**, 896 (2006).
- [7] F. P. Heßberger, S. Hofmann, D. Ackermann, P. Cagarda, R.-D. Herzberg, I. Kojouharov, P. Kuusiniemi, M. Leino, and R. Mann, *Eur. Phys. J. A* **22**, 417 (2004).
- [8] M. Asai *et al.*, *Phys. Rev. Lett.* **95**, 102502 (2005).
- [9] F. P. Heßberger *et al.*, *Eur. Phys. J. A* **29**, 165 (2006).
- [10] T. Ishii, S. Shigematsu, M. Asai, A. Makishima, M. Matsuda, J. Kaneko, I. Hossain, S. Ichikawa, T. Kohno, and M. Ogawa, *Phys. Rev. C* **72**, 021301(R) (2005).
- [11] H. Makii *et al.*, to be published.
- [12] T. Ishii *et al.*, *J. Phys. Soc. Jpn.* **75**, 043201 (2006).
- [13] S. Takeuchi *et al.*, *JAEA-Tokai Tandem Annual Report 2005*, *JAEA-Review 2006-029* (2006), p. 3.
- [14] S. Takeuchi, T. Ishii, M. Matsuda, Y. Zhang, and T. Yoshida, *Nucl. Instrum. Methods Phys. Res. A* **382**, 153 (1996).
- [15] D. M. Brink, *Phys. Lett.* **B40**, 37 (1972).
- [16] K. E. Rehm, D. Frekers, T. Humanic, R. V. F. Janssens, T. L. Khoo, and W. Kutschera, *Physics Division Annual Review*, *ANL-83-25* (1983), p. 91.

- [17] J. Gerl, Ch. Ender, D. Habs, W. Korten, E. Schulz, and D. Schwalm, *Phys. Rev. C* **39**, 1145 (1989).
- [18] F. Rösler, H. M. Fries, K. Alder, and H. C. Pauli, *At. Data Nucl. Data Tables* **21**, 291 (1978).
- [19] *Table of Isotopes*, 8th ed., edited by R. B. Firestone and V. S. Shirley (Wiley, New York, 1996).
- [20] Y. A. Akovali, *Nucl. Data Sheets* **99**, 197 (2003).
- [21] P. Reiter *et al.*, *Phys. Rev. Lett.* **82**, 509 (1999).
- [22] M. Leino *et al.*, *Eur. Phys. J. A* **6**, 63 (1999).
- [23] R.-D. Herzberg *et al.*, *Phys. Rev. C* **65**, 014303 (2001).
- [24] T. H. Braid, R. R. Chasman, J. R. Erskine, and A. M. Friedman, *Phys. Rev. C* **1**, 275 (1970).
- [25] R. R. Chasman, I. Ahmad, A. M. Friedman, and J. R. Erskine, *Rev. Mod. Phys.* **49**, 833 (1977).
- [26] G. Audi, A. H. Wapstra, and C. Thibault, *Nucl. Phys.* **A729**, 337 (2003).
- [27] S. G. Nilsson and I. Ragnarsson, *Shapes and Shells in Nuclear Structure* (Cambridge University Press, New York, 1995) p. 163.
- [28] A. Sobiczewski, I. Muntian, and Z. Patyk, *Phys. Rev. C* **63**, 034306 (2001).
- [29] H. Koura and M. Yamada, *Nucl. Phys.* **A671**, 96 (2000).
- [30] H. Koura, T. Tachibana, M. Uno, and M. Yamada, *Prog. Theor. Phys.* **113**, 305 (2005); [http://www.ndc.tokai-sc.jaea.go.jp/nuclldata/mass/KTUY05\\_m246.dat](http://www.ndc.tokai-sc.jaea.go.jp/nuclldata/mass/KTUY05_m246.dat)
- [31] S. Cwiok, J. Dudek, W. Nazarewicz, J. Skalski, and T. Werner, *Comput. Phys. Commun.* **46**, 379 (1987).
- [32] A. Parkhomenko and A. Sobiczewski, *Acta Phys. Pol. B* **35**, 2447 (2004); **36**, 3115 (2005).